RESEARCH ARTICLE OPEN ACCESS

Mixed carriers thermoelectric effect of vanadium doped ZnTe thin films

M. S. Hossain[1*], M. Nuruzzaman[1], M. A. H. Shah[1], M. Ariful Islam[1]
[1]*Department of Physics, Rajshahi University of Engineering and Technology, Rajshahi-6204, Bangladesh*

ABSTRACT
Vanadium doped zinc telluride (ZnTe:V) thin films (containing 2.5 to 10wt% V) were deposited onto glass substrates by e-beam evaporation technique in vacuum at a pressure of 8×10^{-4} Pa. Thermoelectric power of these films have been measured from room temperature up to 413 K with reference to pure copper material. The deposition rate of the films was maintained at 2.05 nms^{-1}. The composition and temperature dependence thermopower and its related parameters have been studied in detail for a particular thickness of 150 nm. The Fermi levels were determined using a non-degenerate semiconducting model. The carrier scattering index, activation energy and temperature coefficient of activation energy have all been obtained at different ranges of compositions and temperatures. The results of thermopower of ZnTe:V thin films obey an activated conduction mechanism and also suggest that the simultaneous bipolar conduction of both (n- and p-types) carriers (mixed carriers) take place. All these samples are optically transparent and mixed crystalline in structure.

Keywords- Vanadium doped zinc telluride (ZnTe:V), e-beam evaporation, Thermopower, Scattering index, Bipolar conduction , Activation energy

I. INRODUCTION

In recent years, there has been a growing interest in the study of zinc telluride (ZnTe) thin films, as it is a potentially low-cost semiconductor and high absorption co-efficient for application to photovoltaic and photoelectrochemical cells [1-4]. ZnTe has a direct band gap of 2.2 to 2.3 eV at room temperature and usually a p-type semiconductor. Literature [5] report indicates that ZnTe exhibits improved photorefractive response when it is doped with vanadium. Vanadium is believed to be a deep donor in ZnTe and it has attractive use in a variety of applications, including optical power limiting, optical computing and optical communication [6].

Thermoelectric power [TEP] is an effective measurement for explaining the transport mechanism in amorphous as well as crystalline semiconductors. It is the most sensitive quantity to any change or distortion of the Fermi-level in the materials; a measurement of TEP would be a useful option for investigation the electronic conduction in such a sample. Although there have been a number of investigations on the electrical [7, 8], optical [9, 10], electrooptical properties of ZnTe [7, 9, 11] and ZnTe:V [5, 6] films by a number of researchers [5-11], no study is found in the literature on the thermoelectric properties of vanadium doped zinc telluride (ZnTe:V) thin films deposited by e-beam technique. Hence, we have carried out systematic investigation on temperature as well as composition dependence thermopower and its related parameters of ZnTe:V films. It shows that the simultaneous bipolar conduction of both (n- and p-types) carriers i.e. mixed carriers_type conduction take place with temperature and doping of different concentrations of vanadium.

II. EXPERIMENTAL DETAILS

2.1. *Film Preparation*

ZnTe:V thin films have been prepared onto glass substrate by electron bombardment heating technique in vacuum at a pressure of 8×10^{-4} Pa, from a mixture of ZnTe (99.999% pure) and vanadium (99.999% pure), obtained from Aldrich Chemical Company, USA. The ZnTe:V thin films (containing 2.5 to 10 wt% V) of a particular thickness of 150 nm were deposited at a room temperature and their deposition rate was maintained at 2.05 nms^{-1}. Each material of the mixture was weighted by an electrical balance (Mettler TOLEDO, AB 204) having a resolution of ± 0.0001 gm, according to percentage composition to be used. The percentage composition of starting materials in the evaporant mixture (source material), was determined as [12]

$$\text{Weight}\quad \%\,V = \frac{W_V}{W_V + W_{ZnTe}} \times 100\ \% \qquad (1)$$

where W_V and W_{ZnTe} are the weights of V and ZnTe materials, respectively. Then the materials were grinded together using a pestle & mortar and then they are thoroughly mixed. A small quantity of source material was loaded into clean cermet-hearth based on the source turret. Cleaned glass substrate was placed on the substrate-holder at about 0.09 m from the source material. The two masks (one for ZnTe:V films and another for reference copper material) were placed on the mask-holder for the film deposition by e-beam technique. A mechanical shutter was operated from outside, isolated the substrate from the evaporant. The chamber bell jar was thoroughly cleaned with emery paper and cotton wool by wetting acetone and then it was dried with a dryer (model: HP4514) and then placed on the base plate. After completing the steps of operation of the vacuum system, when the chamber pressure reduced to 8×10^{-4} Pa, deposition was then started with e-beam current of 40-50 mA by turning on the low-tension control switch of electron beam power supply (EBS) unit. Details of the film deposition process were reported by author's work [13]. For TEP measurement pure thick copper and also ZnTe:V film were deposited onto glass substrate at room temperature, which is shown in Fig. 1. After completing the deposition, taking them out from the vacuum chamber, the film thickness was determined by the Tolansky interference method [14] with an accuracy of ±5 nm.

ZnTe:V thin films are annealed by a specially designed heater. A flat nichrome wire strip heater covered with mica sheet has been used to heat the film devices. In the heating cycle, the temperature of the film is increased to 473 K, held there for a time of 3 hours and then it is cooled in air. This annealing procedure is maintained for all annealed films. The temperature is measured by a digital thermometer (model: Stk.610-067, England) with chromel-alumel thermocouple placed on the middle of the substrate. The heating and cooling rate is kept at about 10 K/min for each sample. The annealing was necessary because the as-deposited samples were of high order of resistivity.

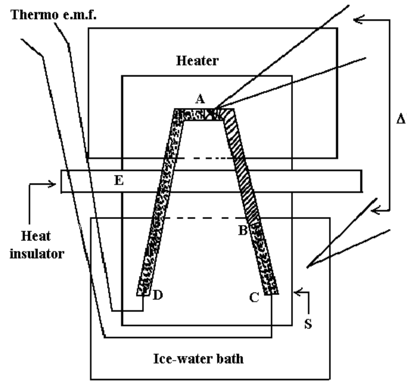

Fig.1. Schematic diagram of thermopower measuring apparatus: AB- ZnTe:V film; AD and BC copper films; S, glass substrate; E, heat insulating barrier and ΔT is the temperature difference between hot and cold ends.

Measurement of TEP was carried out by the integral method [15], in which junction **A** was heated by a nichrome strip heater with regulated power supply to keep it at different temperature. The other junction **B** was immersed in an ice-water bath of constant (273 K) temperature. The temperature of the hot junction was measured by a chromel-alumel thermocouple attached to the sample. The generated thermo e.m.f. was recorded using a Keithley (Model: 614) digital electrometer. The hot and cold junctions were kept thermally isolated by inserting an insulated barrier between the junctions. The immersed portion of the film was kept electrically insulated to remove any leakage of e.m.f. between **D** and **C** due to contact with the ice-water. The whole apparatus was kept in suitable incloser to minimize any air current disturbance. The temperature of the hot junction was raised slowly from room temperature, with a regular interval of 10 K. The thermo e.m.f. was noted up to the highest temperature of 413 K.

III. RESULTS AND DISCUSSION

3.1. Structural Study

The structure of as-deposited and annealed ZnTe:V thin films of a particular thickness of 150 nm for different compositions of 2.5, 5.0, 7.5 and 10wt% V were examined by x-ray diffraction (XRD) technique with the monochromatic Cu-Kα radiation using an apparatus, RINT 2200, Rigaku, Japan. Peak intensities were recorded corresponding to 2θ values.

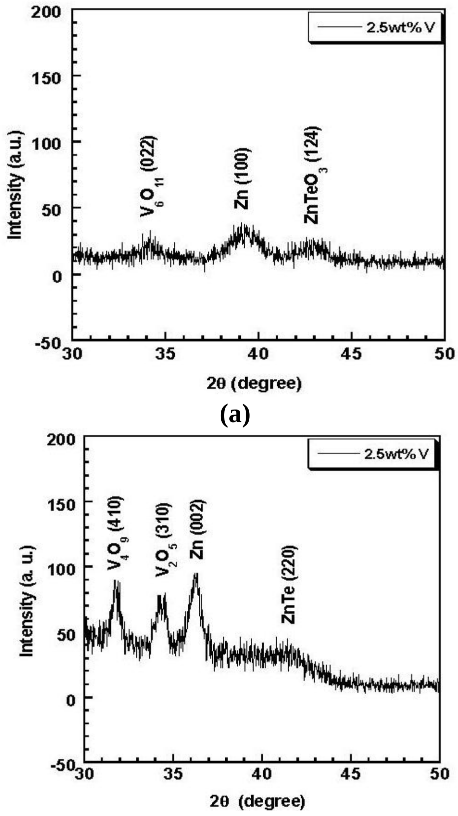

(a)

(b)

Fig. 2. XRD spectra for a 150 nm thick (a) as-deposited and (b) annealed ZnTe:V thin films of composition 2.5wt% V.

Figs. 2(a) and (b) illustrate the XRD spectra of a 150 nm thick as-deposited and annealed ZnTe:V thin films of composition 2.5wt% V onto glass substrate, respectively. In Fig. 2(a) of as-deposited ZnTe:V films, three peaks of 34.16^o, 39.26^o and 42.85^o are observed at 2θ values. These peaks correspond to the phases with plane V_6O_{11} (022), Zn (100) and $ZnTeO_3$ (124), respectively. These phases and planes are found from the JCPDS Cards [16, 17, 18], respectively. For annealed ZnTe:V film of Fig. 2(b), four peaks of 31.67^o, 34.37^o, 36.26^o and 41.69^o are observed at 2θ values, which correspond to V_4O_9 (410), V_2O_5 (310), Zn (002) and ZnTe (220) phases with plane, respectively. These phases and planes are also found from the JCPDS Cards [19, 20, 17, 21], respectively.

In annealed condition, the XRD peaks show up more prominently than that of as-deposited one. This could be attributed to the more crystalline nature of the annealed films. Moreover, the XRD study shows a number of oxide phases present in the author's samples. This oxide phases are formed after deposition by oxygen particles absorbed from the environment replacing one or two of the host elements in ZnTe:V. So, examination of both as-deposited as well as annealed ZnTe:V thin films exhibits the structure of the sample is a mixed crystalline in nature.

3.2. *Surface Morphology Study*

The surface morphology of the as-deposited as well as annealed ZnTe:V thin films for different compositions of a particular thickness were observed by scanning electron microscopy (SEM) using Philips, Model: XL-30, operated at accelerating 10 KV potential.

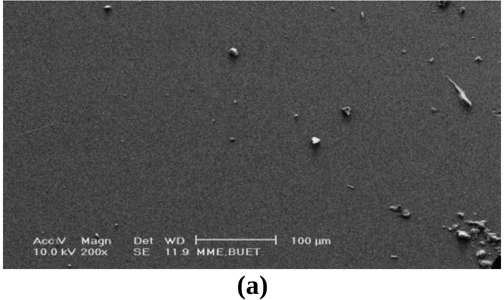

(a)

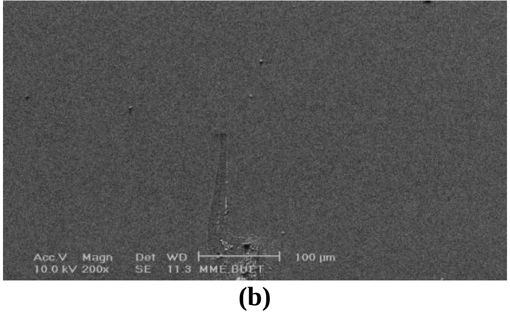

(b)

Fig. 3. SEM micrographs of 100 nm thick (a) as-deposited and (b) annealed ZnTe:V thin films of composition 2.5wt% V.

Figs. 3(a) and (b) show the SEM micrographs of surface morphology for a 100 nm thick as-deposited and annealed ZnTe:V thin films of composition 2.5wt% V, respectively. From both the micrographs, it shows that the film surfaces are dense and compact in nature. In the case of as-deposited ZnTe:V thin film, a few numbers of small-size-dots or pits were observed distributed randomly over the whole sample. After annealing, the dots or pits were removed and a very smooth surface morphology was obtained. From the study of as-deposited and annealed films, it is concluded that the film surfaces of author's samples are dense, smooth and have a compact in nature. Due to the limitation of available SEM system, it was not possible to capture high magnification images of our samples.

3.3. *Elemental Composition Study*

The analysis of the chemical compositions for the as-deposited as well as annealed ZnTe:V thin films of thickness 100 nm were estimated by using the method of energy dispersive analysis of x-ray (EDAX). The results of elemental compositions are shown in Table 1. It is seen from Table 1 that for a 100 nm thick as-deposited and annealed ZnTe:V samples, the elemental composition of V and Zn do increase in annealed case compared to that of as-deposited one whereas, the Te composition is seen to decrease in annealed case. So, the EDAX study suggests that author's ZnTe:V samples are non-stoichiometric in nature.

Table 1. Estimated elemental compositions of V, Zn and Te by EDAX method for 100 nm thick films of 2.5 wt%V.

EDAX results			Remarks
V (wt%)	Zn (wt%)	Te (wt%)	
02.63(±0.51)	41.98(±0.59)	55.39(±1.02)	As-depo.
03.55(±0.41)	42.45(±0.43)	54.00(±1.07)	Annealed

3.4. *Thermopower and Its Related Parameters*

Fig. 4 shows the variation of thermo e.m.f. values at different temperatures for four samples of compositions 2.5, 5.0, 7.5 and 10wt% V, respectively. It is observed that thermo e.m.f. changes in negative up to 343 K and it has then a sharp rise in e.m.f. values till 353 K and above this temperature it has again a linear positive increase with respect to copper for all samples. The region of transition temperature is 10 K and it is termed as anomaly. It may cause due to the properties of transition region formed between films and thermocouple by diffusion or it may cause due to phase deformation of the crystallinity of the studied sample [22]. Fig. 5 shows the variation of thermoelectric power, **S** with the temperature and it is observed that carrier is to be neutral at about 348 K temperature for all the doped samples. From this figure, it is also observed that thermopower decreases in negative up to 343 K, then sharply rises up to 353 K and beyond this temperature thermopower decreases linearly up to 413 K. This figure suggests that n-type carriers and p-type carriers dominate in lower and higher temperature regions in all samples, respectively. All investigated doped samples show the (n- and p-type) mixed-carrier behavior and bipolar in nature.

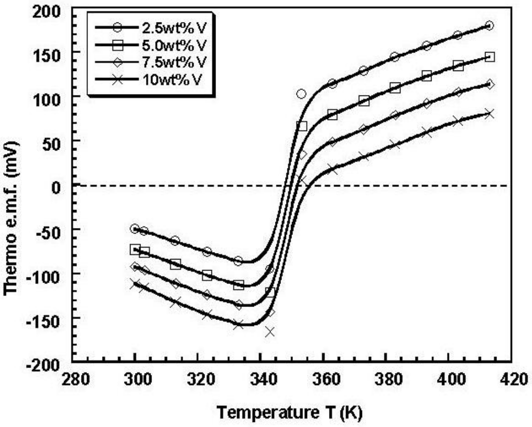

Fig. 4. Thermo e.m.f. vs. temperature curves for ZnTe:V films of different compositions.

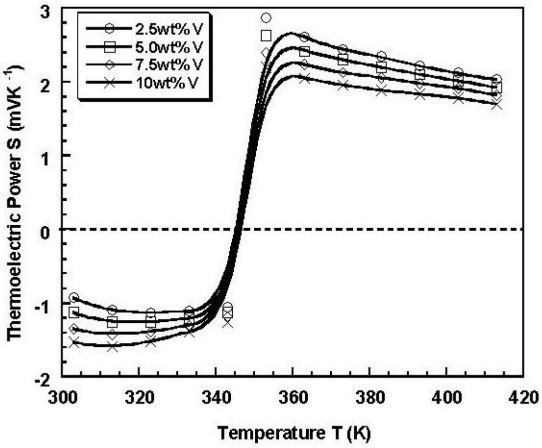

Fig. 5. Thermoelectric power vs. temperature curves for ZnTe:V films of different compositions.

It is separated into two; n-type from 303 to 343 K (termed as below anomaly) and p-type from 353 to 413 K (known as above anomaly) for the more detail study. Figs. 6(a) and (b) show the variation of thermoelectric power with inverse temperature 1/T for below anomaly (n-type carrier) and above anomaly (p-type carrier) temperature, respectively. It is observed from these figures that thermoelectric power decreases continuously with increasing temperature and saturates at higher temperature region.

The rate of change of **S** with temperature is higher for films of higher compositions than that of lower ones. The variation of thermopower **S**, with film compositions of ZnTe:V films are shown in Figs. 7(a) and (b) at a fixed temperature for below anomaly and above anomaly regions, respectively. In the both figures, it indicates that at lower temperature, thermopower has compositions dependence while it is almost compositions independent in higher temperature.

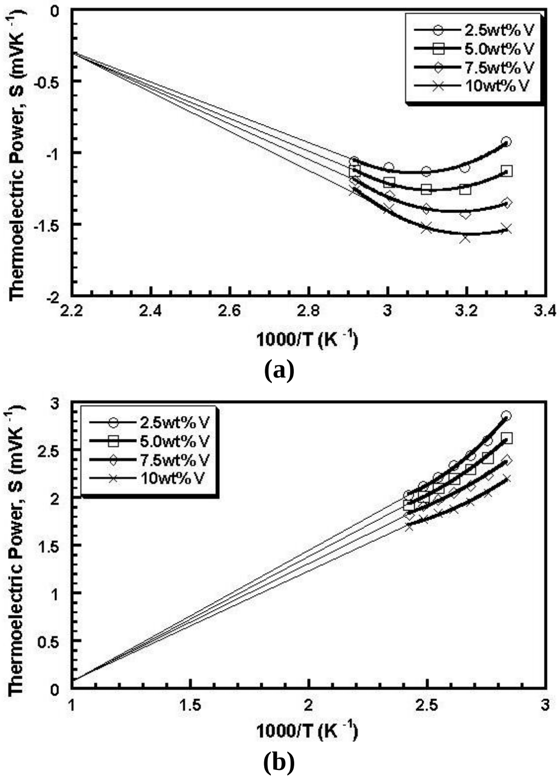

Fig. 6. The plots thermoelectric power vs. inverse temperature curves for (a) below anomaly (b) above anomaly for ZnTe:V films of various compositions.

Because of the very low conductivity in author's sample, it was not possible to measure the Hall coefficient and consequently of their carrier concentration either at room temperature or at any other elevated temperature. So, the free-charge-carrier concentrations have been obtained from thermoelectric measurements.

The thermopower measurement of author's samples gives the value of free-charge-carrier concentration of 2.28×10^{15} -1.72×10^{21} m $^{-3}$ and it is of both n- and p-types. So, it is logical to employ a nondegenerate model [23] to analyze the thermopower data. For a nondegenerate crystalline as well as amorphous semiconductor with spherical constant energy surface under thermal equilibrium, the thermoelectric power is given by the literatures [24-27].

$$S = \pm \frac{k}{e}\left(\frac{E_C - E_F}{kT} + A\right) \qquad (2a)$$

And more generally

$$S = \pm \frac{k}{e}\left(\frac{\Delta E_S}{kT} + A\right) \tag{2b}$$

$$\Delta E_S = (E_F - E_V) \text{ or } (E_C - E_F) \tag{2c}$$

where E_S is thermal energy, E_C is conduction band energy, E_V is valance band energy, E_F is Fermi-level energy and A is a small constant depending on the nature of scattering process of current carriers and its magnitudes varied between 1 and 4 [25, 27]. Harry *et al.* [28] have pointed out that A = (5/2 – r), where r corresponds to the scattering index and is equal to 1.5 for polar scattering of optical phonons supported as many other workers [29-31] and -1 for grain boundary scattering [32]. Thus A = 1 for polar scattering of optical phonons and 3.5 for grain boundary scattering. From Eq. (2b) it is clear that A correspond to a value of the thermopower at infinite temperature limit.

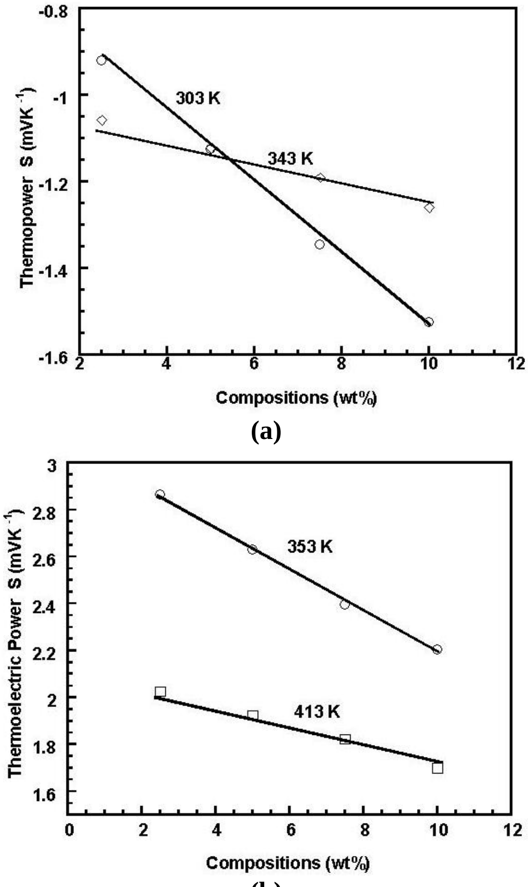

Fig. 7. The variation of thermopower of ZnTe:V films as a function of composition at two different temperatures for **(a)** below anomaly (303 & 343 K) and **(b)** above anomaly (353 & 413 K) temperature, respectively.

From Figs. 6(a) and (b) the extrapolated tangent curves at the higher temperature region give a common intercept at the ordinate S = -0.301 mV/K for below anomaly or n-type and 0.0862 mV/K for above anomaly or p-type carrier, respectively. Putting the values of S in Eq. (2b) the values of A have been obtained as 3.493 and 1.0003, respectively. These values correspond to the scattering index ≈ -1 and ≈ 1.5 are indication of grain boundary and polar scattering of optical phonons which are dominant in these ZnTe:V.

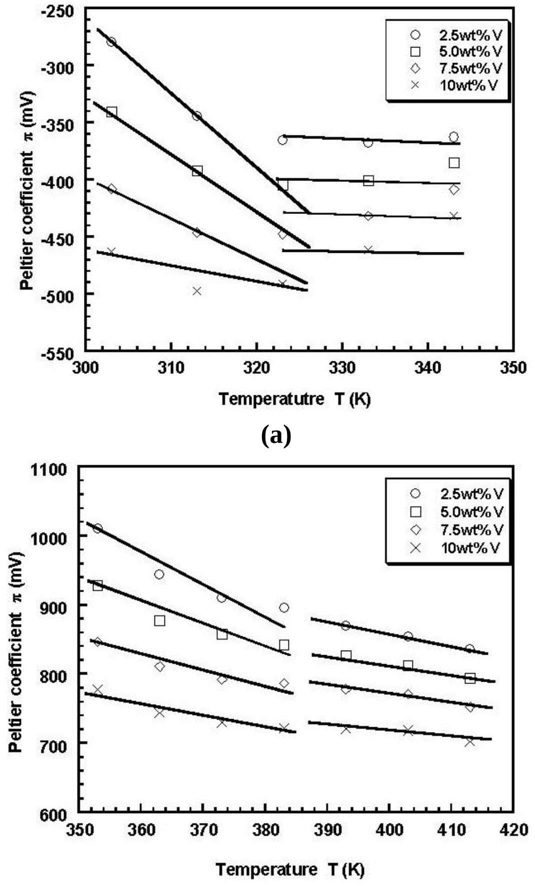

Fig. 8. The plots Peltier coefficient vs. temperature curves for (a) below anomaly (b) above anomaly for ZnTe:V films of various compositions.

In all of the author's samples it has been found that (E_C – E_F) or (E_F – E_V) varies with temperature, T and it can be assumed that for a limited temperature range [33]:

$$(E_C - E_F) \text{ or } (E_F - E_V) = E_o - \gamma T \tag{3}$$

where E_o is the low-temperature limit of ΔE_S and corresponds to the activation energy equivalent to the band gap, γ is the temperature coefficient of activation energy. Putting Eq. (3) into Eq. (2b)

$$S = \pm\left[\frac{E_o}{eT} - \left(\frac{\gamma}{e} - \frac{Ak}{e}\right)\right] \tag{4}$$

Now, the Peltier coefficient π = ST, is given by

$$\pi = \pm\left[\frac{E_o}{e} - \left(\frac{\gamma}{e} - \frac{Ak}{e}\right)T\right] \tag{5}$$

Equation (5) shows that a π versus T plot should yield a straight line and the value of γ can be obtained from its slope. Figs. 8(a) and (b) show such plots and it is observed that the slopes at room and at high temperature (above 323 K) regions are different for below anomaly and that of also found at lower and higher temperature region for above anomaly, respectively. Both slopes have been determined and using A = 3.5 and 1 for n- and p-type respectively, various values of γ were calculated for the ZnTe:V films of different compositions. These values of γ are plotted as a function composition and they are shown respectively in Figs. 9(a) and (b). In both figures, it shows that at higher temperature, γ is almost composition independent while in the room/lower temperature limit; it shows strong composition dependence.

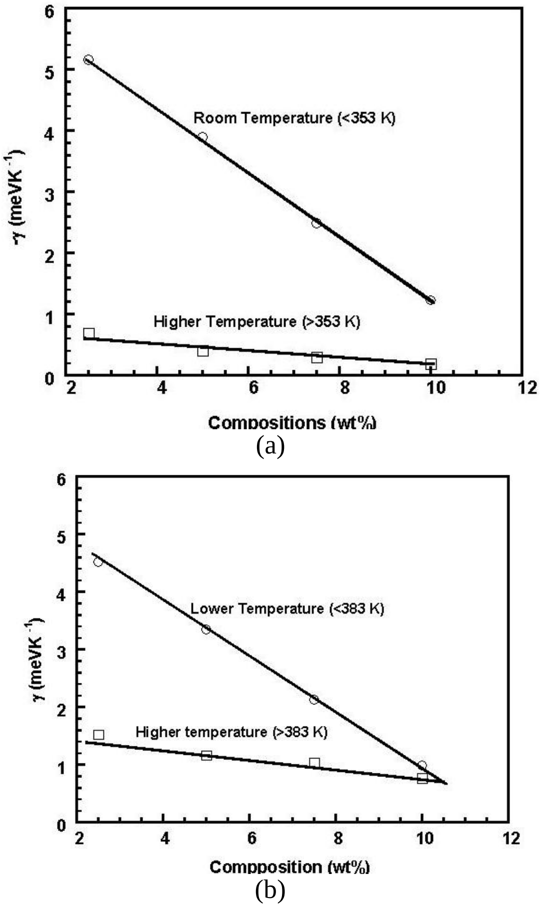

(a)

(b)

Fig. 9. The variation of temperature coefficient of activation energy γ as a function of composition of ZnTe:V films for (a) below anomaly: at room and at higher temperature (above 323 K) (b) above anomaly: at lower and at higher temperature (above 383 K), respectively.

Using these values of γ at room temperature, the values of E_o for the different compositions may be calculated from Eq. (5) and the values of ΔE_S from Eq. (3) for both type carriers. The variations of E_o and of (E_C – E_F) or (E_F – E_V) as a function of inverse compositions, 1/(wt%) at temperature for below and above anomaly are shown in Figs. 10(a) and (b), respectively.

In Figs. 10(a) and (b), it is observed that E_o has fair composition dependence and its trained shows metallic nature corresponding to 1/(wt%) = 0, is almost 0 eV in both graphs. This value does agree well with the metallic properties [34]. In extrinsic samples, the variation of E_o with composition is obvious. E_o is calculated from Eq. (3), is some type of thermal activation energy and depends on the detailed variations of the pattern of the conduction with the structure of the film, including various defects for compositions. This is not necessarily vertical transition. But the optical band gap E_g corresponds to the optical absorption at some frequency and involves mostly vertical transitions between the bands. Thus, the variation of E_g with composition is not so straight forward as for $E_{o,}$ of course, carrier concentration plays an important role in this case.

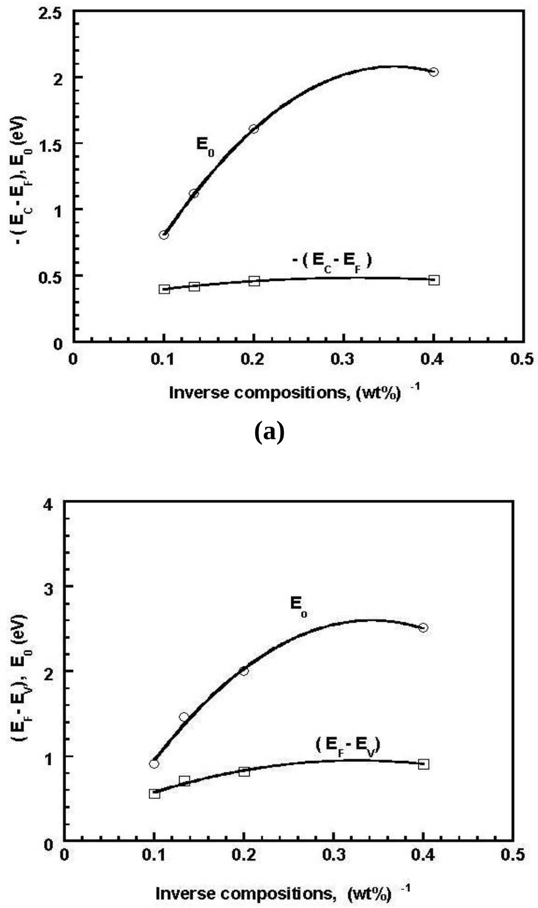

(a)

(b)

Fig. 10. The variation of **(a)** E_o and - (E_C-E_F) for below anomaly **(b)** E_0 and (E_F-E_V) for above anomaly temperature with inverse composition of ZnTe:V thin films.

In the high temperature region, the thermopower saturates for all the samples (Figs. 6 and 7), it suggests that the Fermi-levels in these films are pinned near the mid way at higher temperature. These are now clearly shown in Figs. 11(a) and (b) where the pinning can be clearly observed. All investigated samples for doping show the mixed-carrier behavior and bipolar in nature as in Fig. 5. This behavior means the Fermi level may be formed midway between the conduction and valance band, as discussed by Mott [33]. The gradual decrease of thermopower with temperature for individual n- and p-type which is behaves like a Fermi-glass.

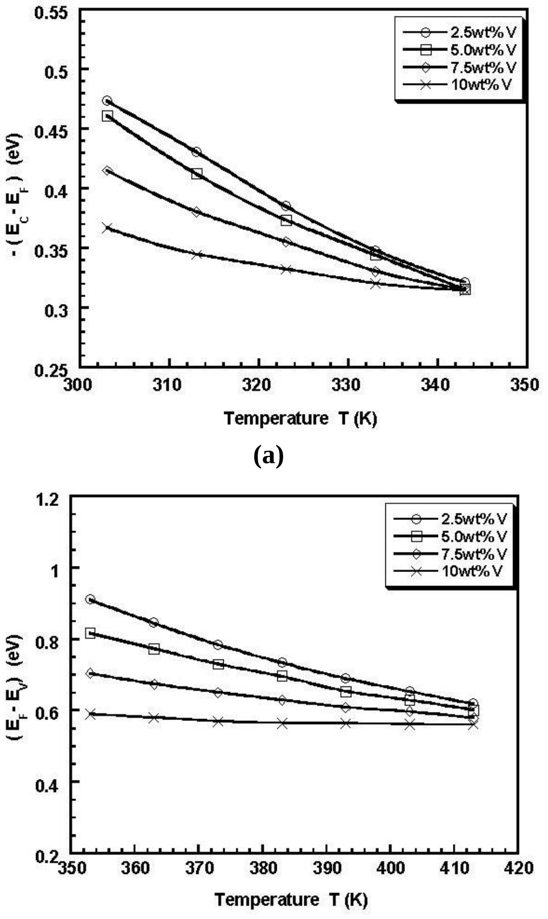

(a)

(b)

Fig. 11. The plots of Fermi-level as a function of temperature for (a) below anomaly (b) above anomaly for ZnTe:V films of various compositions.

We obtain some idea about this variation by differentiating Eq. (2b) with respect to temperature, which yields,

$$\frac{dS}{dT} = \pm \frac{k}{e}\left[\frac{d(\Delta E_s)}{kTdT} - \left(\frac{\Delta E_s}{kT^2}\right) + \frac{dA}{dT}\right] \qquad (8)$$

From Figs. 11(a) and (b), it is observed that for $\Delta E_S = -(E_C - E_F)$, whole term of third bracket of Eq. (8) is positive [35] and for $\Delta E_S = (E_F - E_V)$, whole term of third bracket of Eq. (8) is negative [36] when the change of A is ignored with any possible temperature variation as it corresponds to the higher temperature of thermopower. From the Eq. (8) it is seen that for n-type and p-type concentrations dS/dT is negative as literatures [35, 36], which suggests a decrease of thermopower with temperature, respectively. The minimum value of $-(E_C - E_F)$ and $(E_F - E_V)$ as obtained from Figs. 11(a) and (b) are 0.32 eV and 0.56 eV which are almost 12.18 and 21.7 times that of kT at room temperature. Thus our previous consideration of non-degenerate model to explain the thermopower data is justified.

IV. CONCLUSION

Thermopower in e-beam deposited non-stoichiometric ZnTe:V thin films shows a composition as well as temperature dependence. The Fermi-levels are found to show a pinning mid way between the conduction and valence bands. An annealed as well as the as-deposited vanadium doped sample shows the both carriers (n-type and p-type) thermopower, which supports with previous reported data. In general the transport properties in these samples are controlled by the polar scattering of optical phonons and grain boundary scattering process which corresponding to the scattering index 1.5 and -1, obtained from thermopower data, respectively. Dopant compositions also have a remarkable effect on the activation energy, E_o and on the temperature coefficient of activation energy, γ. In lower temperature region, γ has strong composition dependence while it is almost composition independent in the high temperature region.

ACKOWLEDGEMENT

One of the author's M. S. Hossain is indebted to Rajshahi University of Engineering & Technology, Bangladesh for providing the grants & study leave during this work. He is also grateful to Dr. A. K. M. Farid ul Islam, Physics Department, Govt. Carmichael College, Rangpur, Bangladesh.

REFERENCES

[1] A. Z. Nozik, and R. Memming, Physical chemistry of semiconductor-liquid interfaces, *J. Phys. Chem.* 100, 1996, 13061-13078.

[2] J. O. M. Bockris and K. Uosaki, The rate of photoelectrochemical evolution of hydrogen at p-type semiconductor, *J. Electrochem. Soc.* 124, 1977, 1348-1355.

[3] K. K. Mishra, and K. Rajeshwar, Structural, optical and electrical properties of ZnTe thin films, *J. Electrochem. Soc.* 273, 1978, 169-175.

[4] D. Ham, K. K. Mishra, and K. Rajeshwar, Electrodeposition of PbS, PbSe and PbTe

thin films, *J. Electrochem. Soc*. 138, 1991, 100-106.

[5] M. Ziari, W. H. Steier, and P. M. Ranon, Photorefractivity in vanadium-doped ZnTe, *Appl. Phys. Lett*. 60, 1992, 1052-1054.

[6] J. Kreissl, K. Irmscher, P. Peka, M.U. Lehr, H.-J. Schulz, and U.W. Pohl, Vanadium centers in ZnTe crystals. II. Electron paramagnetic resonance, *Phys. Rev*. B53, 1996, 1917-1926.

[7] -7. H. Dong-Hun, C. Shin-Jung, and P. Su-Moon, Electrochemical preparation of Zinc Telluride films on gold electrodes, *J. Electrochem. Soc*. 150, 2003, C342-C346.

[8] A. K. S. Aqili, Z. Ali, and A. Maqsood, Optical and structural properties of two-sourced evaporated ZnTe thin films, *Appl. Surf. Sci.* 167, 2000, 1-11.

[9] A. Mondal, S. Chaudhuri, and A. K. Pal, Optical properties of ZnTe films, *Appl. Phys. A: Materials Science & Processing* 43, 1987, 81-84.

[10] H. Bellakhder, A. Outzourhit, and E. L. Ameziane, Study of ZnTe thin films deposited by r. f. sputtering, *Thin Solid Films*, 382, 2001, 30-33.

[11] R. L. Gunshor, L. A. Kolodziejski, N. Otsuka, and S. Datta, ZnSe-ZnMnSe and CdTe-CdMnTe super lattices, *Surf. Sci.* 174, 1986, 522-533.

[12] A. S. Khan, *Electrical, optical and micro-structural properties of Ag-Al_2O_3 cermet thin films for solar energy applications*, Ph.D. Thesis, (R.U., Bangladesh, 1999).

[13] M. S. Hossain, R. Islam, and K. A. Khan, Temperature effect on the electrical properties of undoped and vanadium doped ZnTe thin films, *Renewable Energy*, 33, 2008, 642-647.

[14] S. Tolansky, *Multiple Beam Interferometry of Surfaces and Films*, (Oxford University Press, 1948).

[15] V. D. Das, and J. C. Mohanty, Size and temperature effects on thermoelectric power of β-tin thin films. *J Appl Phys.*;54(2), 1983, 977-81.

[16] Andersson, Jahnberg, Arkiv Kemi, JCPDS Card No.18-1451, 21, 1964, 413.

[17] Swansun, Tatge, DC Fel, JCPDS Card No. 4-0831, Reports, 60 (1951).

[18] Frank-Kamenetsky, Univ. of Leningrad, USSR, Saturiwiss, JCPDS Card No. 20-1270, 54, 1967, 199.

[19] W. Karl-Axel, W. Kjell, Acta Chem. Scan., JCPDS Card No.24-1391, 24, 1970. 3409-

[20] Nat. Bur., Standards CIRC, JCPDS Card No.9-387, 8, 1958, 66.

[21] Nat. Bur., Stds. U.S. Mono., JCPDS Card No.15-746, 25, 1964, 58.

[22] K. L. Chopra, *Thin Films Phenomena*, (McGraw-Hill Publ. Co. New York, 1969).

[23] N. W. Ashcroft and N. D. Mermin, *Solid State Physics*, (Holt, Rinehart and Winston Publishers, New York, 1976).

[24] A. Goswami, *Thin Film Fundamentals*, (New Age Int. (P) Lt., Publishers; New delhi, 1996).

[25] H. Fritzsche, *Amorphous and liquid semiconductors*, (Plenum Press, New York, 1971).

[26] H. Fritzsche, The *paper* reports dc conductivity and thermoelectric power (TEP) of a-Se80-xGa20Tex, *Solid State Commun*. 9, 1971, 1813-1821.

[27] Z. H. Khan, M. Zulfeqaur, A. Kumar, and M. Hussain, *Can. J. Phys*. 80, 2002, 19-27.

[28] H. Harry, B. Kwok, and R. H. Bube, Thermoelectric and photothermoelectric effects in semiconductors: CdS single crystals *J. Appl. Phys*. 44, 1973, 138-145.

[29] D. Kranzer, Hall and drift mobility of polar p-type semiconductors. II. Application to ZnTe, CdTe, and ZnSe, *J. Phys. C: Solid State phys.*, 6, 1973, 2977-2987.

[30] H. Tubota, Electrical properties of AIIBVI compounds, CdSe and ZnTe", *Jpn. J. Appl. Phys*. 2, 1963, 259-265.

[31] M. Aven, and B. Segall, Carrier Mobility and Shallow Impurity States in ZnSe and ZnTe, *Phys. Rev*., 130, 1963, 81-91.

[32] K. N. Raju, R. P. Vijayalakshmi, R. Vanugopal, D. R. Reddy, and B. K. Reddy, Effect of substrate temperature on structural, optical and electrical properties of vacuum-evaporated ZnTe films, *Materials Letters*, 13, 1992, 336-341.

[33] N. F. Mott and E. A. Davis, *Electronic Processes in Non-Crystalline Materials*, *2nd Edn. Clarendon Press, Oxford, UK, 47, 48, 235, 271 & 273 (1979).*

[34] K. Kase, Electroabsorption in ZnTe Doped with In or Al, *Jpn. J. Appl. Phys*. 17, 1978, 1805-1812.

[35] A. K. M. Farid UL Islam, R. Islam, and K. A. Khan, *J. Mater. Sci.: Mater. in Electronics*, 16, 2005, 203-.

[36] M. S. Hossain, R. Islam, M. Shahjahan, and K. A. Khan, Studies on the thermoelectric effect in semiconducting ZnTe thin films, *J Mater Sci: Mater Electron*. 19, 2008, 1114–1121.